molecular pharmaceutics

Article

pubs.acs.org/molecularpharmaceutics

Elucidating the Mechanisms Behind Sonoporation with Adeno-Associated Virus-Loaded Microbubbles

Bart Geers,[†] Ine Lentacker,[†] Angelika Alonso,[‡] Niek N. Sanders,[§] Joseph Demeester,[†] Stephen Meairs,[‡] and Stefaan C. De Smedt*,[†]

[†]Ghent Research Group on Nanomedicines, Lab of General Biochemistry and Physical Pharmacy, Faculty of Pharmaceutical Sciences, Ghent University, Harelbekestraat 72, 9000 Gent, Belgium

[‡]Department of Neurology, Universitätsklinikum Mannheim, Heidelberg University, Theodor-Kutzer-Ufer 1-3, 66167 Mannheim, Germany

[§]Laboratory of Gene Therapy, Faculty of Veterinary Medicine, Ghent University, Heidestraat 19, 9820 Merelbeke, Belgium

Supporting Information

ABSTRACT: Microbubbles are Food and Drug Administration (FDA) approved contrast agents for ultrasound imaging. It has been reported that applying ultrasound on drug-loaded microbubbles facilitates drug uptake by cells, due to so-named sonoporation. However, the biophysics behind sonoporation are not fully understood. It is believed that sonoporation results in a "direct" delivery of drugs in the cytoplasm of cells, though it has been suggested as well that sonoporation facilitates endocytosis which would improve the internalization of drugs by cells. To get a better understanding of sonoporation, this study reports on the ultrasound assisted delivery of adeno-associated virus (AAV) loaded on the surface of microbubbles. AAVs rely on endocytosis for efficient transduction of cells and are, consequently, an elegant tool to evaluate whether endocytosis is involved in ultrasound-induced sonoporation. Applying ultrasound on AAV-loaded microbubbles clearly improved the internalization of AAVs by cells, though transduction of the cells did not occur, indicating that by sonoporation substances become directly delivered in the cytosol of cells.

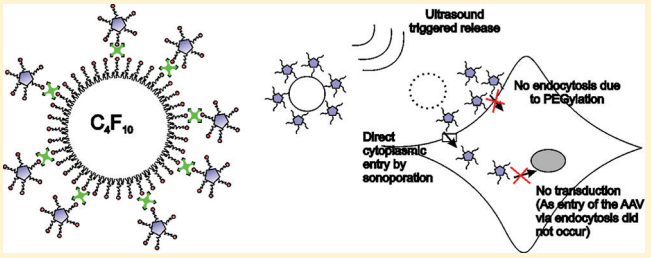

KEYWORDS: *ultrasound, microbubbles, sonoporation, AAV, PEGylation*

INTRODUCTION

For a few years, interest in microbubbles as drug delivery carriers has grown exponentially. A major reason for this is that microbubbles, with some of them being approved by the Food and Drug Administration (FDA) as contrast agents for diagnostic ultrasound, may allow time and space controlled drug delivery upon mechanical activation of the bubbles by ultrasound.[1] Such micrometer-sized bubbles are usually filled with an inert hydrophobic gas, while their shell consists out of lipids, polymers, or proteins.[2,3]

The mechanism of action of these microbubbles is based on the specific response of the bubbles upon exposure to ultrasound.[4] Because of the difference in density between the gas core of the microbubble and the surrounding aqueous fluid, microbubbles start to oscillate once subjected to the pressure fluctuations as exerted by an ultrasonic wave. This process of oscillation is called cavitation.[5] "Stable cavitation" occurs when microbubbles are subjected to an ultrasonic field with a low acoustical pressure (i.e., acoustical pressure that does not induce microbubble implosion); stably cavitating microbubbles expand and contract around a given diameter. "Inertial cavitation" on the other hand involves a more violent process: the bubbles do not longer oscillate around a given diameter and become destroyed.[6] It has been shown that cell membranes neighboring a cavitating or collapsing microbubble may become transiently permeabilized ("sonoporation")[7] which is believed to enhance the cellular uptake of drugs.

However, the biophysics behind this mechanism is not yet fully understood. Our group showed that when drug molecules are attached to the microbubble surface, microbubble collapse promotes the direct delivery of these drug molecules into the cytosol of the surrounding cells.[8] However, other studies described that sonoporation might induce the formation of endocytic vesicles which could also explain the more efficient drug uptake by cells when exposed to ultrasound.[9] Hence, there is a need to further elucidate the biophysical effects involved in sonoporation, which is the objective of this paper. To prove if sonoporation involves endocytosis or not, we studied the transduction of cells by means of adeno-associated virus (AAV) as a vector, which totally relies on receptor-mediated endocytosis to successfully transduce cells.[10,11] More specifically, we

Received: March 8, 2011
Revised: October 13, 2011
Accepted: October 20, 2011
Published: October 20, 2011

made use of "non-active AAV", which are AAV vectors chemically modified at their surface with a poly(ethylene glycol) (PEG) brush. This PEGylation strongly reduces the endocytosis of AAV vectors and, subsequently, lowers their transduction properties.[12,13] We believe that such PEGylated AAV vectors are an ideal tool to study whether endocytosis is involved in the sonoporation process as a better transduction of the cells upon applying ultrasound and microbubbles would become only observed if ultrasound promotes endocytosis. Since our research group is mainly focusing on lipid-shelled microbubbles,[14−16] we decided for the purpose of this study to bind PEGylated AAV vectors to lipid-shelled microbubbles through Avidin−biotin linkages, as illustrated in Figure 1A.

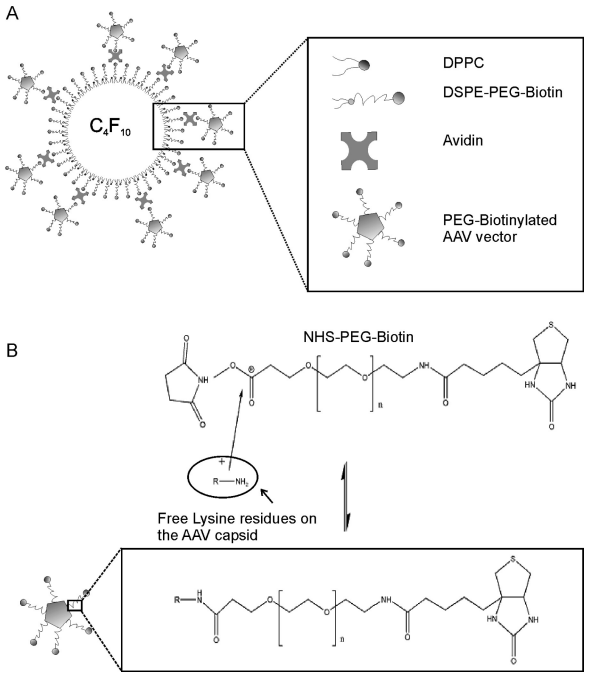

Figure 1. (A) Schematic representation of an AAV-loaded microbubble. The microbubble consists of a pefluorobutane (C_4F_{10}) gas core, surrounded by a lipid monolayer containing 1,2-dipalmitoyl-*sn*-glycero-3-phosphocholine (DPPC) and 1,2-distearoyl-*sn*-glycero-3-phosphoethanolamine-*N*-biotinyl(polyethylene glycol)-2000] (DSPE-PEG-biotin). Via avidin−biotin bridging, PEG-biotinylated AAV vectors were loaded on the surface of the microbubbles. (B) Chemical coupling of PEG-biotin molecules to the viral capsid. The α-biotin-ω-carboxy succinimidyl ester poly(ethylene glycol) (NHS-PEG-biotin) reagent interacts with amine groups on lysine residues present on the AAV capsid and binds PEG-biotin molecules onto the viral capsid through an amide bond.

EXPERIMENTAL SECTION

Preparation and Characterization of Biotinylated Microbubbles. Microbubbles were prepared following the protocol published by Lentacker et al.[15] Briefly, the phospholipids 1,2-dipalmitoyl-*sn*-glycero-3-phosphocholine (DPPC) and 1,2-distearoyl-*sn*-glycero-3-phosphoethanolamine-*N*-biotinyl(polyethylene glycol)-2000] (DSPE-PEG-BIOTIN) (Avanti polar lipids, Albaster, AL) both dissolved in $CHCl_3$ were added in a round-bottom flask in an 85:15 molar ratio. After $CHCl_3$ evaporation, the lipid film was dissolved in 4-(2-hydroxyethyl)-1-piperazineethanesulfonic acid (HEPES) buffer 50 mM, pH 7.4 (Sigma-Aldrich, Bornem, Belgium). This mixture was extruded using a 200 nm polycarbonate membrane filter in a mini-extruder (Avanti Polar Lipids, Albaster, AL) at 60 °C to obtain liposomes with a minimal size of 200 nm, as measured by dynamic light scattering (Nanozs, Malvern, Worcestershire, UK). An aliquot of the liposomal dispersion was transferred into a 15 mL tube, and subsequently C_4F_{10} gas (MW 238 g/mol, F2 chemicals, Preston, UK) was added to this dispersion. Microbubbles could be obtained by ultrasonication of the liposomes with a 20 kHz probe (Branson 250 sonicator, Branson Ultrasonics, Danbury, CT). After sonication the microbubbles were centrifuged for 5 min at 300 g to remove the remaining liposomes. Microbubbles were washed with 3 mL of HEPES buffer. To allow coupling of biotinylated AAV vectors, the microbubbles were subsequently incubated with 500 μL of avidin (10 mg/mL) for 5 min at room temperature. After another washing step with 3 mL of HEPES buffer and subsequent centrifugation (5 min, 300 g), microbubbles were incubated with biotinylated AAV vectors. The microbubble concentration was evaluated using light microscopy in a Burker chamber and equaled 1×10^7 microbubbles per mL.

Preparation and Characterization of PEG-Biotinylated AAV Vectors. Recombinant adeno-associated virus serotype 2 (rAAV2) expressing enhanced green fluorescent protein (EGFP) was provided by the German Cancer Research Centre, with a stock concentration of 10^{12} particles/mL. To obtain PEGylated or PEG-biotinylated AAV vectors, a 100 μL aliquot of the AAV vectors was incubated with a desired amount of α-methoxy-ω-carboxylic acid succinimidyl ester poly(ethylene glycol) (MW 2000 g/mol, Iris Biotech GmbH, Marktdrewitz, Germany) (NHS-MPEG2000) or α-biotin-ω-carboxy succinimidyl ester poly(ethylene glycol) (NHS-PEG-biotin) (MW 3000 g/mol, Iris Biotech Gmbh, Marktredwitz, Germany) respectively. Therefore, the NHS-MPEG2000 or NHS-PEG-biotin were dissolved in HEPES buffer (1 mg/mL) just before adding to the AAV-vector dispersion. The vectors were incubated with the PEGylation agent for 30 min at room temperature. Subsequently HEPES buffer was added to obtain a final volume of 300 μL with a concentration of 5×10^{10} particles/mL. PEGylation of the AAV was characterized by measuring the electrophoretic mobility of the viral particles with a zetasizer (Nanozs, Malvern, Worcestershire, UK).

Preparation of Fluorescent AAV Vectors. AAV vectors were fluorescently labeled with red- or green-fluorescent labels. For labeling in red, 100 μL of PEG-biotinylated AAV vectors (freshly prepared) were incubated with 3−5 μL of NHS-dyelight633 labeling reagent (2 mg/mL, Thermo Scientific, Bornem, Belgium) for 30 min. After incubation the dye excess was removed by dialysis against distilled water (MWCO 15000 Da, Microdispo dialyser, Spectra/Por, Compton, CA). Green-fluorescent AAV vectors were obtained by labeling 100 μL of PEG-biotinylated AAV vectors (freshly prepared) with 3−5 μL of NHS-alexa488 (2 mg/mL, Invitrogen Molecular Probes, Merelbeke, Belgium).

Preparation and Characterization of AAV-Loaded Microbubbles. AAV-loaded microbubbles were prepared by mixing 3 mL of PEG-biotinylated microbubbles with 300 μL of the PEG-biotinylated AAV vectors. To remove unbound AAV vectors, microbubbles loaded with the AAV vectors were washed with 3 mL of HEPES- buffer and centrifuged for 5 min at 300 g twice. The percentage of vectors present in the subnatans after every centrifugation step was analyzed with an AAV titration ELISA assay (Progen GmbH, Heidelberg, Germany).

The remaining bubble fraction after these washing steps was then dispersed in 3 mL of HEPES, and the amount of AAV vectors bound to the microbubbles was analyzed with the same assay. We quantified the amount of AAV vectors on the microbubbles to ensure that in all experiments the same vector titers were used.

To visualize AAV loading on the microbubbles, the microbubbles were incubated with alexa488-avidin (Invitrogen Molecular Probes, Merelbeke, Belgium) and mixed with red-fluorescent PEG-biotinylated AAV vectors. Colocalization of (green) avidin and (red) AAV was studied by confocal microscopy, using a Nikon EZC1 confocal microscope (Nikon, Brussels, Belgium) equipped with a 60× water immersion objective with a numerical aperture of 1.2. Excitation of the alexa488 avidin was done using the 488 nm line of the Ar-ion laser, while fluorescence was detected at 551 nm. Excitation of the AAV vectors labeled with the red NHS-dyelight633 dye was done using the 630 nm line of the diode-pumped solid-state laser, while fluorescence was detected at 660 nm.

Cell Culture. BLM cells (melanoma cells) were cultured in F12-supplemented Dulbecco's modified Eagle's medium (DMEM-F12). This medium also contained 1% penicillin/streptomycin, 2 mmol/mL L-glutamine, 10% fetal bovine serum (FBS) (all purchased from Gibco, Merelbeke, Belgium), and 100 mmol/L HEPES pH 7.2. Cells were grown in an humidified incubator at 37 °C in a 5% CO_2 atmosphere.

Transduction of Melanoma Cells with PEGylated AAV-Vectors. BLM melanoma cells were seeded at 1.3×10^6 cells and grown up to 70% confluency in Opticell plates (Biocrystal, Westerville, OH). Before the transduction medium was added, cells were washed with 10 mL of phosphate buffered saline (PBS). AAV vectors were PEGylated as described above using 20, 40, 100, and 200 μg of NHS-MPEG2000. A sample of 200 μL of PEGylated rAAV2 expressing EGFP was added to 9.8 mL of cell culture medium and transferred into the Opticells; afterward cells were incubated for 45 min at 37 °C. Subsequently cells were washed with 10 mL of PBS, fresh cell culture medium was added, and cells were incubated. After 48 h cells were washed and incubated for 10 min at 37 °C with 2 mL of a 0.05% trypsin-EDTA solution (GIBCO, Merelbeke, Belgium), after 5 min of incubation trypsin was inactivated with 8 mL of fresh culture medium and centrifuged for 7 min at 300 g. Subsequently medium was removed, and cells were resuspended in buffer containing 1% of bovine serum albumin and 0.1% of sodium azide in PBS (chemicals were purchased from Sigma-Aldrich, Bornem, Belgium). EGFP expression was measured using flow cytometry with a BD Facscalibur flow cytometer (Beckton Dickinson, Erembodegem, Belgium). The flow cytometer was equipped with a 488 nm laser, and emitted fluorescence was detected in the 530 nm channel FL1. Results are expressed as % EGFP positive cells compared with blank untransducted cells. All experiments were performed at least in triplicate, and data are expressed as the mean of all three measurements.

Cytotoxicity Assay. BLM melanoma cells were seeded in 12-well plates at 1×10^5 cells and grown up to 70% confluency. Cells were washed, and 10 μL of free AAV or inactive PEGylated AAV with a stock concentration of 10^{12} particles/mL dispersed in cell medium to a final volume of 1 mL was added to the cells. PEGylation occurred via the method described above. Subsequently, cells were incubated for 24 h at 37 °C in a 5% CO_2 atmosphere. After incubation, cells were washed with PBS, and afterward 50 μL of MTT-reagent (Roche, Leuven, Belgium) dissolved in cell medium up to 500 μL was added to the cells; subsequently cells were incubated for 4 h at 37 °C in a 5% CO_2 atmosphere. Finally, 500 μL of solubilization reagent was added. The next day, cell viability was determined by measuring the absorbance of the formed formazan. The absorbance of each plate was measured in an absorbance plate reader at respectively 590 nm to determine the formed formazan and at 690 nm as a reference. The results of the cytotoxicity measurements are expressed as percentages; the viability of the cells which were only treated with cell medium was considered to be 100%, while the viability of cells exposed to DMSO was considered to be 0%. Experiments were performed in triplicate.

Transduction of Melanoma Cells with AAV-Loaded Microbubbles and Ultrasound. BLM melanoma cells were seeded at 1.3×10^6 cells and grown up to 70% confluency in Opticell plates as mentioned above. Microbubbles were loaded with rAAV2 vectors expressing EGFP, which were first PEG-biotinylated using 20 or 100 μg of NHS-PEG-BIOTIN, according to the method described above. Control experiments were performed using respectively non-PEGylated AAV vectors and "free" PEGylated AAV vectors (i.e., not bound to microbubbles). In each transduction experiment the same AAV concentration was used. After washing the cells, 1 mL of AAV-loaded microbubbles, with a concentration of approximately 1×10^7 microbubbles per mL, was mixed with 9 mL of fresh culture medium and added to the cells. Subsequently, Opticell plates were submerged in a warm water bath (37 °C) with a bottom of ultrasound absorbing rubber. The ultrasound was delivered by manually moving a Sonitron ultrasound probe over the whole plate during 10−15 s. We used 1 MHz ultrasound with a 10% duty cycle, and the ultrasound intensity was $2W/cm^2$. After 45 min of incubation at 37 °C, microbubbles were removed, and cells were washed with 10 mL of PBS and incubated in fresh culture medium at 37 °C in a 5% CO_2 atmosphere. At 48 h later, cells were trypsinized, centrifuged, and resuspended in flow buffer for flow cytometry analysis as described above. Results were expressed as % EGFP positive cells compared with untreated cells. All experiments were performed at least in triplicate, and data are expressed as the mean of all three measurements.

Internalization of AAV in Melanoma Cells Treated with AAV-Loaded Microbubbles and Ultrasound. BLM cells were grown under the conditions as described above. For these experiments microbubbles were loaded with green Alexa488-labeled rAAV2 and PEG-biotinylated using 100 μg of NHS-PEG-biotin and 1 mL of bubbles (1×10^7 microbubbles/mL). The AAV-loaded microbubbles were dispersed in fresh culture medium and added to the Opticells. Subsequently, Opticell plates were subjected to ultrasound as described above. Cells were washed, and fresh culture medium was added. The intracellular localization of the green-fluorescent AAV vectors was analyzed 15 min after ultrasound application by confocal microscopy using the 488 nm laser line as described above. The cells were analyzed as well by flow cytometry as described above. However, before flow cytometry analysis, to quench extracellular fluorescence cells were incubated with Trypan blue for 10 min at room temperature. After incubation cells were washed with 10 mL of PBS and trypsinized as described above.

Colocalization of Endosomes with Inactive AAV Vectors Loaded on Microbubbles after Ultrasound Application. BLM melanoma cells were grown under the

conditions described above and transferred in Opticell plates. Endosomal labeling was performed by means of transduction with the BacMam 2.0 Cellight Reagent (Invitrogen, Merelbeke, Belgium). Briefly, the cells were washed with PBS, and according to the manufacturer's recommandations, 150 μL of BacMam 2.0 reagent together with 9.85 mL of cell medium was subsequently added to the cells. Afterward the cells were incubated for 24 h at 37 °C under 5% CO_2 atmosphere.

Before the ultrasound experiments, microbubbles were prepared as described above and loaded with red-fluorescent labeled inactive PEGylated AAV. PEGylation of the vectors was performed as described in previous sections using 100 μg of NHS-PEG-biotin, and the vectors were fluorescently labeled with 2 μL of NHS-dyelight633 (2 mg/mL). These fluorescent AAV-loaded microbubbles were supended in cell medium, and this mixture was added to the cells. Subsequently, the Opticell plates were subjected to the same ultrasound conditions as used in the other ultrasound experiments. The cells were visualized with confocal microscopy as described above, 15 min post insonation using both the 488 nm laser line and the 633 nm laser line.

Statistical Analysis. All data are presented as means ± one standard deviation. A Student's t test was performed to determine whether data sets differed significantly. A p-value smaller than 0.05 was regarded significant.

RESULTS

Design of an AAV-Loaded Microbubble Using PEG-Biotinylated AAV. Figure 1A schematically shows the structure of the AAV-loaded microbubbles we designed. The microbubbles consist of a lipid shell, composed of the phospholipids DPPC and DSPE-PEG-biotin, which surrounds a perfluorobutane gas core. The presence of biotin-containing lipids allowed the coupling of PEG-biotinylated AAVs through an avidin linker. Therefore the AAV vectors were chemically modified making use of the NHS-PEG-biotin reagent. As shown in Figure 1B, amine groups on lysine residues on the viral capsid and succimidin ester groups in the NHS-PEG-biotin reagent are involved in this reaction with the formation of amide bonds as a result.

To confirm successful PEGylation of the AAV vectors, we measured the ζ-potential of the AAV vectors respectively before and after the PEGylation reaction; note that NHS-MPEG instead of NHS-PEG-biotin was used in these experiments. As shown in Figure 2, the PEGylation reaction clearly increased the ζ-potential of the AAV vectors, indicating that PEG molecules shielded the negative charges on the viral capsid. As only a (relatively) low amount of NHS-MPEG per amine present on the viral capsid was used, the PEGylation of the AAV vectors through the NHS coupling strategy seems to be an efficient process.

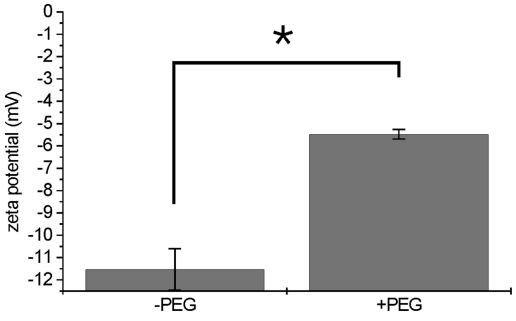

Figure 2. ζ-potential measurements on non-PEGylated AAV vectors (−PEG) and PEGylated AAV vectors (+PEG). The higher ζ-potential of the PEGylated AAVs indicates a successful coupling of NHS-MPEG to the viral capsid. PEGylation was performed using 15 μg of NHS-MPEG per 5×10^{10} viral particles (*$p < 0.05$).

In the next step we tried to load the lipid microbubbles with the PEG-biotinylated AAV vectors. The successful loading of the AAV vectors on the microbubbles' surface was confirmed by confocal microscopy. Figure 3 shows that green-fluorescent avidin binds to the surface of biotinylated lipid microbubbles (Figures 3B). Binding of the red-fluorescent PEG-biotinylated AAV vectors to the microbubbles is shown in Figure 3C. Figure 3D clearly shows colocalization of green-labeled avidin and red-labeled AAV vectors on the microbubble's surface proving loading of microbubbles with AAV vectors through avidin−biotin linkages.

Influence of PEGylation of AAV Vectors on Their Transduction Properties and Cytotoxicity. To evaluate the influence of PEGylation on the transduction efficiency of the AAV vectors we made use of EGFP expressing rAAV2 vectors. By flow cytometry we measured the percentage of EGFP positive cells as a function of the PEGylation degree of the AAV vectors. Therefore, AAV vectors were PEGylated using increasing amounts of PEG, ranging from 20 to 200 μg NHS-MPEG per 5×10^{10} viral particles. As can be seen in Figure 4A, the transduction efficiency of the AAV vectors became clearly impaired if more than 40 μg of PEG reagent was used. Using 20 μg of NHS-MPEG, the PEGylated AAVs were still able to transduct approximately 10% of the cell population.

To exclude the possibility that these reduced transduction rates are due to an enhanced toxicity of the PEGylated AAV vectors, we analyzed the viability of cells treated with these PEGylated AAV vectors. As shown by Figure 4B, indeed some significant cytotoxicity could be observed in cells treated with inactive PEGylated AAV. However, still more than 80% of the cells remained perfectly viable after this treatment. We can hence conclude that reduced transduction rates observed are not due to the cytotoxicity of these PEGylated vectors.

These results, however, indicate that PEGylation of AAV vectors itself hampers their transduction efficiency. Because the PEG brush is expected to shield the viral capsid proteins thereby preventing optimal interactions with cell membrane components which is essential for their receptor-mediated internalization (see below).

Since we wanted to investigate the effect of sonoporation on endocytosis, we considered to perform our further experiments with AAV vectors that were not able to transduce cells on their own, that is, "inactive vectors" (being vectors which were strongly PEGylated through the use of 100 μg of PEG-reagent per 5×10^{10} viral particles). As Figure 4A shows, these inactive (strongly PEGylated) vectors are completely incapable to transduce cells, likely due to the fact that they could no longer be endocytosed.

Internalization of AAV in Melanoma Cells Treated with Inactive AAV-Loaded Microbubbles and Ultrasound. As shown in Figure 5, we quantified the internalization of inactive AAVs (loaded on microbubbles) in melanoma cells, in the presence and the absence of ultrasound, using flow cytometry: a clear shift in overall fluorescence of the cells could be observed if ultrasound was applied. These results indicate that most cells show a significant internalization of vectors when ultrasound was applied, while there was no internalization

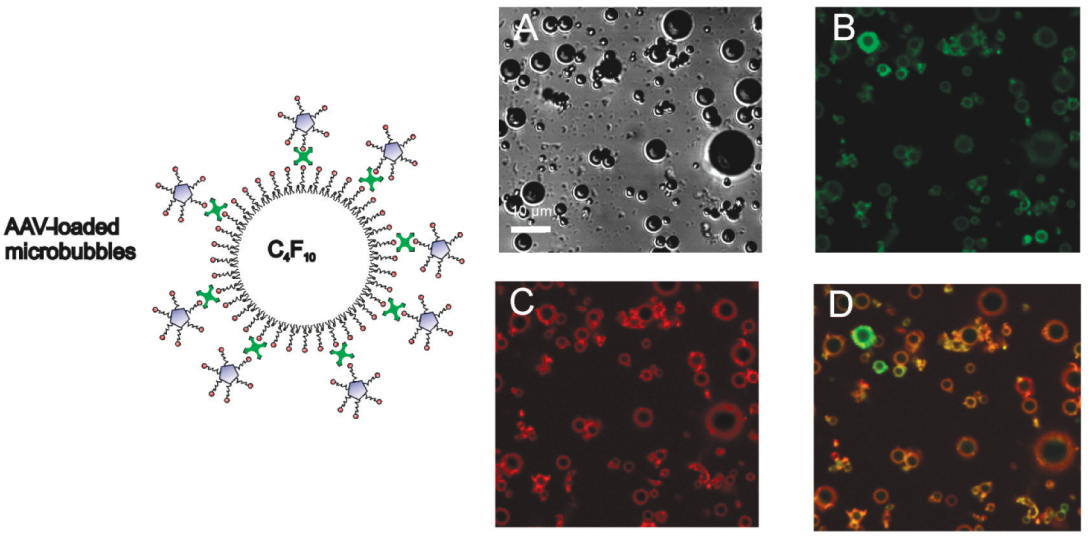

Figure 3. Transmission images of AAV-loaded microbubbles (A). Confocal images show green-labeled avidin (B) and red-labeled AAVs (C) on the surface of the microbubbles. A clear colocalization can be observed between red-labeled AAV and green-labeled avidin (D).

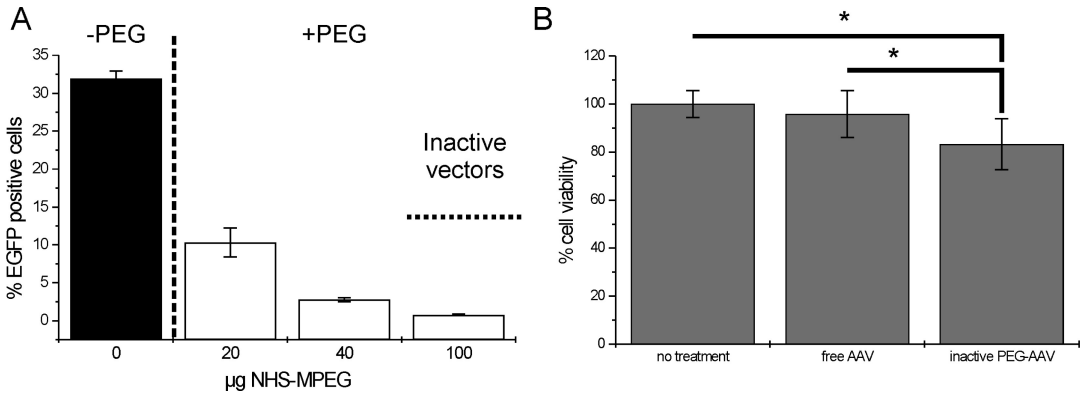

Figure 4. (A) Percentage of EGFP positive cells after transduction with (free) non-PEGylated AAV (black bar) and (free) PEGylated AAV vectors (white bars). PEGylation of the AAV vectors was performed with respectively 20, 40, 100, and 200 μg of NHS-MPEG per 5×10^{10} particles. (B) Cell viability of melanoma cells after transduction with free AAV and inactive PEGylated AAV compared with no treatment (*$p < 0.05$).

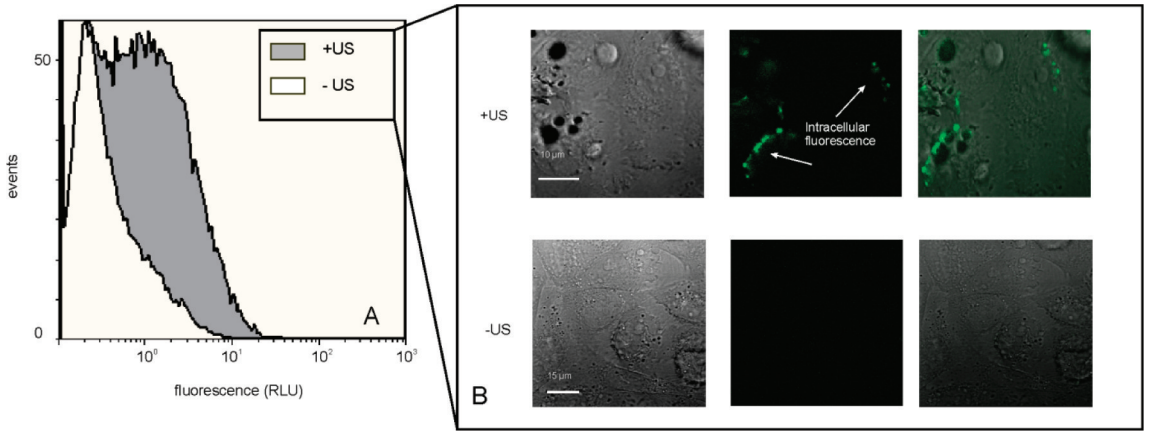

Figure 5. (A) Cellular internalization of green fluorescent inactive PEGylated AAV vectors loaded on microbubbles with (+US) and without ultrasound (−US) radiation, as studied by flow cytometry. Remark that the extracellular fluorescence of the melanoma cells was quenched with Trypan blue. Results show the fluorescence of the cells (RLU) in function of the number of cells counted by the flow cytometer ("events"). (B) Confocal and transmission images and an overlay of both confocal and transmission images of cells treated with green fluorescent inactive PEGylated AAV vectors loaded on microbubbles respectively with (+US) and without (−US) applying ultrasound.

without ultrasound. To confirm the internalization data obtained by flow cytometry experiments, we performed confocal microscopy making use of green fluorescent inactive PEGylated AAV vectors loaded on microbubbles. Panel B in Figure 5 shows

enhanced fluorescence in the ultrasound treated cells, clearly confirming the flow cytometry observations.

Influence of Ultrasound and Microbubbles on Transduction of Cells by Inactive AAV. As Figure 5 showed clear cellular uptake of the PEGylated AAVs upon applying ultrasound, we measured subsequently the transduction efficiencies of AAV-loaded microbubbles (Figure 6). As described in the Experimental Section, we first determined the amount of AAV that became loaded on the surface of the microbubbles to make sure that the cells were exposed to the same amount of vectors as used in the transduction experiments with free virus in Figure 4A. We observed that applying ultrasound to PEGylated AAVs bound to microbubbles does not result in efficient transduction of the cells, suggesting that ultrasound does not promote endocytosis. To exclude the possibility that ultrasound damaged the AAV vectors' DNA or the capsid proteins, experiments with active PEGylated AAV (i.e., PEGylated AAV vectors still capable in transducing cells) were performed (Supporting Information, Figure S2). These experiments showed that ultrasound did not affect the transduction properties of the AAV vectors since we observed significant transduction after ultrasound.

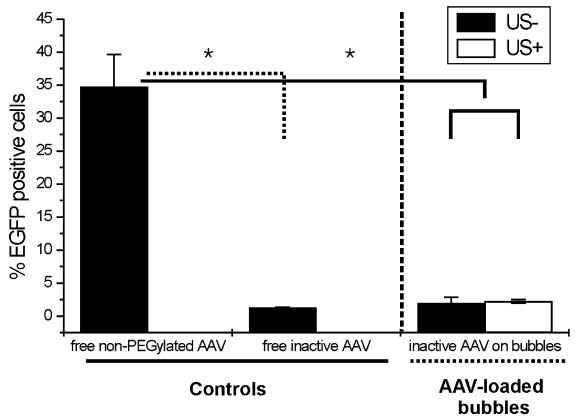

Figure 6. Percentage of EGFP positive cells, as measured by flow cytometry, after transduction of melanoma cells with AAV-loaded microbubbles in the presence (white bars) and absence (black bars) of ultrasound. As a control free non-PEGylated AAV vectors were used and compared with free PEGylated AAV (black bars) (*$p < 0.05$).

Combining the internalization (Figure 5) and transduction data (Figure 6), we can conclude that (a) ultrasound clearly enhances internalization of AAV vectors loaded on the surface of the bubbles, while (b) this does not induce an efficient transduction. We believe that there is no transduction because ultrasound does not deliver the AAV vectors into the cells through endocytosis, being the natural entry pathway of AAVs which is essential for the efficient transduction of the cells.

Endosomal Colocalization Studies To Confirm Direct Cytoplasmic Delivery upon Ultrasound. To really confirm the hypothesis that ultrasound evades endocytosis as suggested by the internalization and transduction experiments, confocal microscopy on cells with labeled endosomes needed to be performed. As described in the Experimental Section, cells were transducted using the BacMam 2.0 technique. This technique allows transduction of a GFP-reporter gene targeting the Rab5a sequence which is specific for early enodosomes. After staining, the cells were exposed to microbubbles loaded with red-fluorescent labeled inactive AAV vectors, and ultrasound was applied. Directly after ultrasound application, we performed microscopy, and we specifically checked for any colocalization between red and green fluorescence.

As shown in Figure 7 we could not observe any significant colocalization of these red-labeled vectors with the green-labeled endosomes, since no merged green and red (orange) signals could be observed inside the cells. Consequently these data clearly show that ultrasound enables direct delivery of the particles loaded on the surface of the bubbles in the cytosol of the cell without endosomal internalization.

DISCUSSION

Earlier studies indicated that an enhanced deposition of drug molecules in cells through the use of microbubbles and ultrasound relies on the formation of transient pores in the cell membrane which arise upon implosion of the microbubbles.[7] Recently we suggested that nanoparticles (like nucleic acid containing lipoplexes) which are attached to the surface of microbubbles become "directly" delivered in the cytosol of cells upon imploding the bubbles with ultrasound, thus avoiding internalization of the nanoparticles through endosomes.[8] In contrast, other groups suggested that sonoporation enhances endocytosis.[9] In the present study we used PEGylated AAV-loaded microbubbles to elucidate the cellular entrance mechanism behind sonoporation. Shielding the viral capsid with PEG chains makes AAV vectors impossible to interact with cell membrane receptors essential in receptor-mediated endocytosis. This blocks cellular transduction, as AAV capsids have to become exposed to endosomal acidification (which enhances their phospholipase activity) to be active.[10,17]

Figure 8 illustrates our hypothesis which explains what might happen during and right after microbubble collapse. Exposing AAV-loaded microbubbles to ultrasound will cause the implosion of the microbubbles and subsequent membrane perforation (sonoporation). Since the only pathway causing successful transduction of the AAV vectors is endocytosis and since we did not observe any transduction of the cells while the AAV vectors were clearly delivered in the cells without endosomal uptake, we hypothesize that ultrasound enables direct entry of the AAV vectors in the cytoplasm. This method of internalization, however, cannot result in an efficient transduction of the internalized AAV vectors.

It is clear that these results are of importance for ultrasound-induced drug delivery since it limits the usage of some viral vectors for gene delivery. If an enhancement of endocytosis is needed for the effect of a certain gene-delivery system, it will not be compatible with this mechanism. On the other hand, this direct cytoplasmic delivery can enhance the delivery of nanoparticles that are sequestered by endocytic vesicles.

Allthough the results in this report are based on results with one particular viral vector and at specific ultrasound settings, we suggest that sonoporation enables direct access to the cell cytoplasm. However, we believe that (a) the ultrasound parameters used may cause different effects on cells and (b) that it cannot be excluded that sonoporation enhances endocytosis in other particular cases, which may explain observations and conclusions in other studies. In this study we used ultrasound parameters that are destructive for the microbubbles, as we could visually observe. With such ultrasound intensities and provided microbubble collapse occurs in the vicinity of cells, the cell membrane becomes perforated due to microjets, microstreams, and shockwaves.[21] The results presented in this paper suggest that these processes will promote

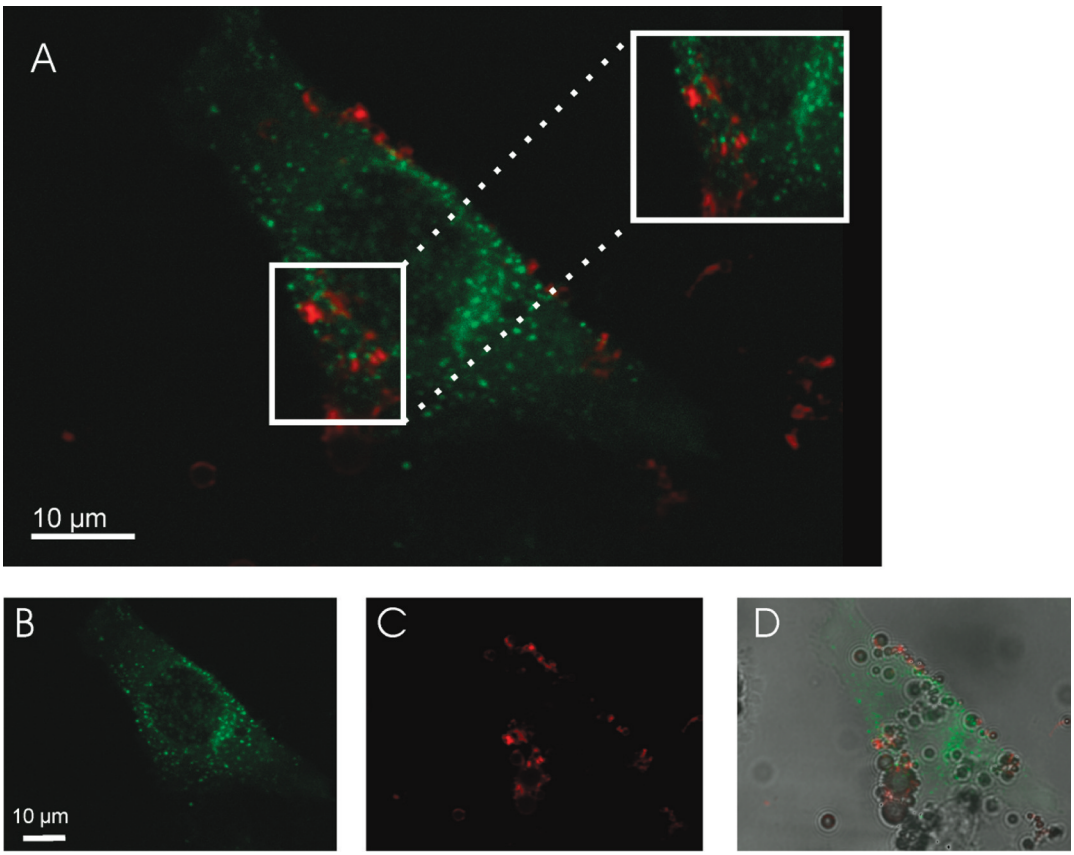

Figure 7. Confocal images of green-labeled endosomes merged with red-labeled inactive AAV vectors (A) the inlet shows a magnification of a region with a high density of red-labeled vectors inside the cell. B and C respectively show confocal images of green-labeled endosomes inside the cell and red-labeled inactive AAV vectors. D shows a transmission image merged with confocal images of green and red fluorescence. Note that some bubbles remain attached to the cell after insonation.

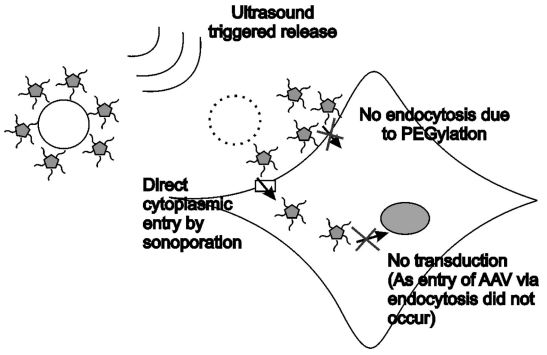

Figure 8. Schematic representation of ultrasound-mediated internalization of PEGylated AAV vectors loaded on microbubbles. Sonoporation will cause direct cytoplasmatic entry of the inactive AAV vectors.

direct cytoplasmic entry of particles attached on the surface of the microbubble. However, at lower ultrasound intensities, microbubbles will stably oscillate. If this oscillation occurs in the vicinity of cells, the movement of the bubbles gently massages the cell membrane. This phenomenon is shown in different studies by Van Wamel et al.,[18−20] and it is possible that this process does induce endocytosis.[9]

■ ASSOCIATED CONTENT

Supporting Information

Internalization of free inactive-PEGylated AAV and free AAV and transduction of active PEGylated AAV-loaded microbubbles. This material is available free of charge via the Internet at http://pubs.acs.org.

■ AUTHOR INFORMATION

Corresponding Author

*Mailing address: Ghent University, Laboratory of General Biochemistry and Physical Pharmacy, Harelbekestraat 72, 9000 Gent, Belgium. Tel.: +32 9 264 80 76. Fax: +32 9 264 81 89. E-mail: stefaan.desmedt@ugent.be.

■ ACKNOWLEDGMENTS

This work was funded by the EU FP7 collaborative projects ARISE (which is a part of the European Stroke Network), SONODRUGS (NMP-4-LA-2008-213706), and the FWO-Vlaanderen research project G.0187.11. I.L. is a postdoctoral fellow of the FWO Flanders research fund (FWO-Vlaanderen).

■ REFERENCES

(1) Hernot, S.; Klibanov, A. L. Microbubbles in ultrasound-triggered drug and gene delivery. *Adv. Drug Delivery Rev.* **2008**, *60* (10), 1153−1166.

(2) Lentacker, I.; De Smedt, S. C.; Sanders, N. N. Drug loaded microbubble design for ultrasound triggered delivery. *Soft Matter* **2009**, *5* (11), 2161−2170.

(3) Stride, E. Physical principles of microbubbles for ultrasound imaging and therapy. *Cerebrovasc. Dis.* **2009**, *27* (Suppl 2), 1−13.

(4) Sboros, V. Response of contrast agents to ultrasound. *Adv. Drug Delivery Rev.* **2008**, *60* (10), 1117−1136.

(5) Wu, J.; Nyborg, W. L. Ultrasound, cavitation bubbles and their interaction with cells. *Adv. Drug Delivery Rev.* **2008**, *60* (10), 1103–1116.
(6) Newman, C. M. H.; Bettinger, T. Gene therapy progress and prospects: Ultrasound for gene transfer. *Gene Ther.* **2007**, *14* (6), 465–475.
(7) Mehier-Humbert, S.; Bettinger, T.; Yan, F.; Guy, R. H. Plasma membrane poration induced by ultrasound exposure: implication for drug delivery. *J. Controlled Release* **2005**, *104* (1), 213–222.
(8) Lentacker, I.; Wang, N.; Vandenbroucke, R. E.; Demeester, J.; De Smedt, S. C.; Sanders, N. N. Ultrasound Exposure of Lipoplex Loaded Microbubbles Facilitates Direct Cytoplasmic Entry of the Lipoplexes. *Mol. Pharmaceutics* **2009**, *6* (2), 457–467.
(9) Meijering, B. D.; Juffermans, L. J.; van Wamel, A.; Henning, R. H.; Zuhorn, I. S.; Emmer, M.; Versteilen, A. M.; Paulus, W. J.; van Gilst, W. H.; Kooiman, K.; de Jong, N.; Musters, R. J.; Deelman, L. E.; Kamp, O. Ultrasound and microbubble-targeted delivery of macromolecules is regulated by induction of endocytosis and pore formation. *Circ. Res.* **2009**, *104* (5), 679–687.
(10) Bartlett, J. S.; Wilcher, R.; Samulski, R. J. Infectious entry pathway of adeno-associated virus and adeno-associated virus vectors. *J. Virol.* **2000**, *74* (6), 2777–2785.
(11) Ding, W.; Zhang, L.; Yan, Z.; Engelhardt, J. F. Intracellular trafficking of adeno-associated viral vectors. *Gene Ther.* **2005**, *12* (11), 873–880.
(12) Le, H. T.; Yu, Q. C.; Wilson, J. M.; Croyle, M. A. Utility of PEGylated recombinant adeno-associated viruses for gene transfer. *J. Controlled Release* **2005**, *108* (1), 161–177.
(13) Lee, G. K.; Maheshri, N.; Kaspar, B.; Schaffer, D. V. PEG conjugation moderately protects adeno-associated viral vectors against antibody neutralization. *Biotechnol. Bioeng.* **2005**, *92* (1), 24–34.
(14) Lentacker, I.; De Geest, B. G.; Vandenbroucke, R. E.; Peeters, L.; Demeester, J.; De Smedt, S. C.; Sanders, N. N. Ultrasound-responsive polymer-coated microbubbles that bind and protect DNA. *Langmuir* **2006**, *22* (17), 7273–7278.
(15) Lentacker, I.; De Smedt, S. C.; Demeester, J.; Van Marck, V.; Bracke, M.; Sanders, N. N. Lipoplex-loaded microbubbles for gene delivery: A Trojan horse controlled by ultrasound. *Adv. Funct. Mater.* **2007**, *17* (12), 1910–1916.
(16) Lentacker, I.; Geers, B.; Demeester, J.; De Smedt, S. C.; Sanders, N. N. Design and Evaluation of Doxorubicin-containing Microbubbles for Ultrasound-triggered Doxorubicin Delivery: Cytotoxicity and Mechanisms Involved. *Mol. Ther.* **2010**, *18* (1), 101–108.
(17) Hansen, J.; Qing, K.; Srivastava, A. Adeno-associated virus type 2-mediated gene transfer: altered endocytic processing enhances transduction efficiency in murine fibroblasts. *J. Virol.* **2001**, *75* (9), 4080–4090.
(18) van Wamel, A.; Kooiman, K.; Harteveld, M.; Emmer, M.; ten Cate, F. J.; Versluis, M.; de Jong, N. Vibrating microbubbles poking individual cells: Drug transfer into cells via sonoporation. *J. Controlled Release* **2006**, *112* (2), 149–155.
(19) van Wamel, A.; Bouakaz, A.; Versluis, M.; de Jong, N. Micromanipulation of endothelial cells: ultrasound-microbubble-cell interaction. *Ultrasound Med. Biol.* **2004**, *30* (9), 1255–1258.
(20) van Wamel, A.; Kooiman, K.; Emmer, M.; ten Cate, F. J.; Versluis, M.; de Jong, N. Ultrasound microbubble induced endothelial cell permeability. *J. Controlled Release* **2006**, *116* (2), e100–e102.
(21) Ohl, C. D.; Arora, M.; Ikink, R.; de Jong, N.; Versluis, M.; Delius, M.; Lohse, D. Sonoporation from jetting cavitation bubbles. *Biophys. J.* **2006**, *91* (11), 4285–4295.